Mode Conversion Due to Discontinuities in Modified Grounded Coplanar Waveguide

Robert W. Jackson

Department of Electrical and Computer Engineering
University of Massachusetts
Amherst, MA 01003

Abstract

Modified grounded coplanar waveguide is the same as conventional grounded coplanar waveguide except that the side planes are not of infinite extent. This structure is overmoded, but is still used in monolithic circuits since it does not require via holes. In this paper, conversion from the desired CPW mode to an undesirable microstrip–like mode is calculated using a full wave analysis. Results indicate that this conversion can be made small for reasonable structural dimensions.

Introduction

The recent use of grounded coplanar waveguide in monolithic circuits [1] has renewed interest in this type of circuit medium for monolithic millimeter wave applications. Grounded coplanar waveguide (GCPW) differs from conventional coplanar waveguide (CPW) by the addition of a ground plane on the underside of the substrate. This improves heat removal at some expense to the range of impedance values which are possible [2]. Both GCPW and CPW have the advantages which result from having all RF circuitry and grounds on one side; elimination of via holes, simplified construction, and reduced parasitic inductance. Both also have low dispersion and potentially low loss [3].

In ideal CPW and GCPW, the top side (and bottom side for GCPW) ground planes extend to infinity. For the GCPW this creates a region which supports a parallel plate wave. Since this wave is slow compared to the desired CPW mode, it serves as a vehicle for energy leakage [3], [4], [5].

For practical MMIC's, the ground planes do not extend to infinity and this radically affects the GCPW leakage. In this paper, we consider the "modified" grounded coplanar waveguide illustrated in Figure 1. The modified structure differs from the conventional structure in that S_2 is finite instead of infinite. For small values of S_2, there are three modes which propagate on this line; the CPW mode (Figure 1a), a parasitic microstrip–like mode (Figure 1b), and a mode with odd symmetry (not shown). As S_2 increases, more and more parasitic modes can propagate until, for infinite S_2, a continuum of parasitic (parallel plate) modes are possible. In this paper, the side plane dimension, S_2, is limited such that only the three lowest order modes can propagate. For many practical structures this is still a fairly large dimension ($\sim \lambda_0/(4\sqrt{\epsilon_r})$). Furthermore, only symmetric structures will be considered so that the CPW mode can only excite the parasitic microstrip mode. This is a reasonable assumption since air bridges are normally used to short out the mode with odd symmetry.

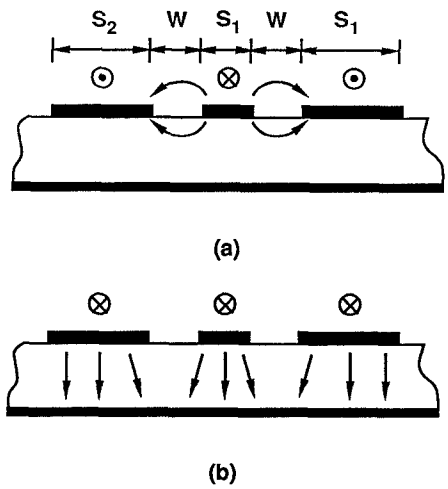

Figure 1. Modified grounded coplanar waveguide; (a) CPW mode currents and fields, (b) microstrip–like mode currents and fields.

For an infinitely long line on GCPW, there is always a parasitic parallel plate wave whose velocity can match the velocity of the desired CPW mode. Coupling and leakage will therefore occur. In the modified GCPW considered here, the single parasitic mode, for typical frequencies, does not travel at the CPW mode velocity. Therefore, coupling does not occur on the uniform line. It does, however, occur at discontinuities just as coupling can occur at discontinuities in an overmoded rectangular waveguide. One type of discontinuity which will couple to the parasitic mode occurs when the modified GCPW is fed at the substrate edge [1]. Another type occurs when shorts or steps in the modified GCPW take place on the substrate surface. The latter will be studied herein.

0149-645X/88/0000-0203$01.00 © 1988 IEEE

In this work, a rigorous numerical technique is used to investigate the coupling between a CPW mode and the microstrip–like mode at a short circuit discontinuity in modified GCPW. The short circuit discontinuity is illustrated in Figure 2. A CPW wave which is incident on this type of discontinuity results in two waves being reflected, the desired CPW mode and the parasitic mode. In what follows, the numerical technique will first be described. Representative results will then be presented.

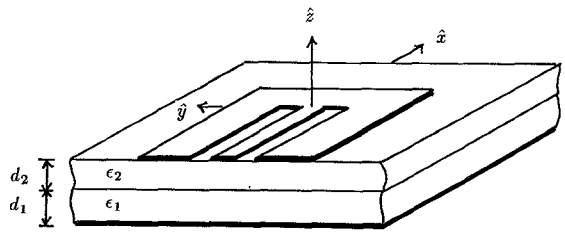

Figure 2. Modified coplanar waveguide short circuit supported by two dielectrics over a ground plane.

Theory

A rigorous application of the method of moments is used to analyze this problem. The procedure is similar to methods developed in references [6], [7], [8], and especially [9]. A Green's function was developed for the substrate configurations shown in Figure 2. The figure shows a two–dielectric slab which extends to $\pm$ infinity in the x and y directions. A ground plane is present on the underside. The incident transmission line is modified GCPW if $d_1 = 0$. No top cover is assumed, although adding one would be a minor modification. The Green's function relates the x and y components of the electric field on the top surface to the surface current, $\vec{J}$, on the same surface,

$$\vec{E}(x,y) = \frac{1}{(2\pi)^2}\int_{-\infty}^{\infty} \vec{\vec{Q}}(k_x,k_y)\cdot \cdot \vec{J}(k_x,k_y)e^{jk_x x}e^{jk_y y}dk_x dk_y \qquad (1)$$

where $\vec{E}(x,y)$ is the two component surface field, $\vec{J}(k_x,k_y)$ is the Fourier transform of the surface current, and $\vec{\vec{Q}}(k_x,k_y)$ is the Fourier transform of the Green's function for a current element located at the origin. The expression for $\vec{\vec{Q}}$ has been published elsewhere [10] and will not be repeated here. The current, $\vec{J}$, is expanded as follows,

$$\vec{J} = \sum_{j=1}^{NM} A_j \vec{J}_j^{fe} + R_{MS}\vec{J}^{RMS} + R_{CP}\vec{J}^{RCP} + \vec{J}^{ICP} \qquad (2)$$

where $\vec{J}^{RMS}$, $\vec{J}^{RCP}$ and $\vec{J}^{ICP}$ are precomputed sinusoidal currents which have known forms (propagation constants, y dependence, x and y current components) and which correspond to the reflected microstrip–like mode, the reflected CPW mode and the incident CPW mode respectively. The $\vec{J}_j^{fe}$ are finite element rooftop currents, some of which are x–directed and some y–directed. NM is the total number of finite elements, and A_j, R_{MS}, R_{CP} are complex coefficients which are to be determined. Weighted averages of the tangential electric field on the CPW surface are set to zero according to

$$-\iint_{-\infty}^{\infty} \vec{W}_i(x,y)\cdot\vec{E}(x,y)dxdy = 0 \qquad i = 1,2,3,...NM+2. \qquad (3)$$

where $\vec{W}_i$ are the weighting functions which, except for two, are the same as the finite element expansion currents. The resulting matrix has the form,

$$\left[\vec{\vec{Z}}\right]\cdot\begin{bmatrix}\vdots\\ A_j\\ \vdots\\ R_{MS}\\ R_{CP}\end{bmatrix} = -\left[\vec{Z}_I\right] \qquad (4)$$

where the $\vec{\vec{Z}}$ matrix results from testing the first three types of expansion functions in (2) and the vector $\vec{Z}_I$ results from testing the current $\vec{J}_{ICP}$. These impedances are carefully evaluated in order to take into account surface wave and space wave effects. Equation (4) is then solved for the unknown coefficients.

There are two types of expansion functions and two types of weighting functions used in this analysis. Rooftop functions [6], [7] are used for expansion and weighting in the junction area while precomputed sinusoids are used to model the incident and reflected waves which extend away from the junction [9]. Two additional weighting functions are used at the edge of the finite element region. These additional functions are x–directed and extend across the width of the CPW and both have triangular x dependence. One has a y variation consistent with the microstrip–like mode and the other has a y variation consistent with the CPW mode (see g_x^{CP}, g_x^{MS} below).

The incident and reflected precomputed sinusoids have the form,

$$\underset{\rightarrow}{J}^{ICP} = \left[g_x^{CP}(y)\hat{x} + jg_y^{CP}(y)\hat{y}\right] \cdot \cdot \left[\cos(\beta^{CP}x) - j\sin(\beta^{CP}x)\right] \quad (5a)$$

$$\underset{\rightarrow}{J}^{RCP} = \left[g_x^{CP}(y)\hat{x} - jg_y^{CP}(y)\hat{y}\right] \cdot \cdot \left[\cos(\beta^{CP}x) + j\sin(\beta^{CP}x)\right] \quad (5b)$$

$$\underset{\rightarrow}{J}^{RMS} = \left[g_x^{MS}(y)\hat{x} - jg_y^{MS}(y)\hat{y}\right] \cdot \cdot \left[\cos(\beta^{MS}x) + j\sin(\beta^{MS}x)\right] \quad (5c)$$

where the propagation constants β^{MS}, β^{CP} and the functions, $g_x^{CP}, g_y^{CP}, g_x^{MS}, g_y^{MS}$ are computed from a full wave analysis of the infinite line. Pulse functions are used in modeling g_x while triangular functions are used to model g_y. The sizes of these pulses and triangle functions are commensurate with the rooftop functions used in the junction area. In the discontinuity calculation, the x dependence of (5) is truncated as described in [9].

Once the coefficients R_{MS} and R_{CP} in (3) are determined, they are adjusted to represent ratios of the total center strip currents for the different modes. The power/current impedance of each mode is defined with respect to those currents. Using this impedance (calculated in a separate routine) the ratio of reflected microstrip–like mode power to incident CPW mode power is finally computed.

Results

In the results that follow, the short circuit discontinuity is modeled as shown in the inset to Figure 3, except that the element density is usually roughly double what is shown. For x–directed currents, the elements have a triangular x dependence which extends over a distance, $W_s/2$ and a pulse y dependence of extend, $S_1/4$. For y–directed currents, the elements have a pulse x dependence extending over a distance $W_s/4$ and a triangular y dependence which spans a distance of $S_1/2$. The finite element region extends back from the short ($x < 0$) by over a slot width. At the lowest frequencies, the number of y divisions was halved. By varying the number and size of the elements, it is estimated that the results are converged to within 10% of the exact value.

As stated previously, a CPW wave which is incident on this junction reflects into a CPW mode and a microstrip–like mode (Figure 1a and b). The CPW–to–CPW reflection coefficient (R^{CP}), as expected, is consistent with an inductive short circuit. If a microstrip–like mode is launched at the discontinuity, the MS–to–MS reflection coefficient (not R^{MS}) is, as expected, consistent with a capacitive open circuit. Plots of the current on the short circuit show that the current bunches along the $x = 0$ edge, as it should.

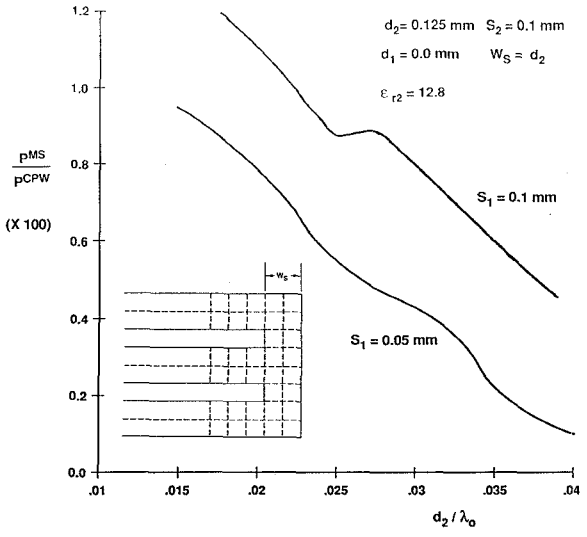

Figure 3. Fraction of incident CPW power converted to MS–like reflected power plotted versus frequency.

Figure 3 shows a plot of the fraction of incident CPW power which is reflected into the microstrip–like mode as a function of frequency for two different impedance modified GCPW lines. The converted power is less than 1.2 percent of the incident power. Increasing frequency results in decreasing mode conversion.

Figure 4 shows a plot of the fractional power converted as a function of the CPW size for a fixed frequency and substrate thickness. Larger sizes increase the fraction of power converted up to the point where the center strip width is about equal to the substrate thickness.

An open–circuited modified GCPW was also examined. Referring to Figure 2, the open circuit was formed by extending the slots all the way to the end of the line. Mode conversion in this case was so small that it is beyond the capability of the analysis to accurately calculate it.

Conclusions

The analysis presented in this work is concerned with a particular type of discontinuity over a limited range of parameters.

The results so far indicate that mode conversion in modified grounded coplanar waveguide occurs at discontinuities, but that it is a small effect. Still, in very high Q circuits, resonances may occur due to this coupling. A more complete study of this configuration (increasing W_S, for example) may show increased coupling as a result of tuning effects.

Coupling to the parasitic microstrip–like mode at the transition on to a chip may be the most significant source of parasitic modes. This problem has not yet been investigated.

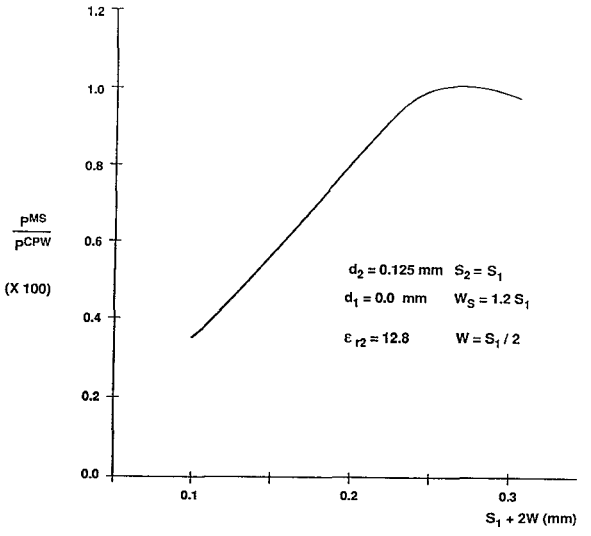

Figure 4. Fraction of incident CPW power converted at 60 GHz for a fixed substrate thickness plotted versus modified GCPW size.

References

[1] M. Riaziat, et al., "Coplanar Waveguide Used in a 2–18 GHz Distributed Amplifier," IEEE MTT–S Microwave Symposium Digest, 1986, pp. 337–338.

[2] Pucel, R. A., "Design Considerations for Monolithic Microwave Circuits," IEEE Trans., MTT–29, 1981, pp. 513–534.

[3] Jackson, R. W., "Considerations in the Use of Coplanar Waveguide for Millimeter Wave Integrated Circuits," IEEE Trans., MTT–34, 1986, pp. 1450–1456.

[4] Oliner, A. A. and K. S. Lee, "The Nature of the Leakage from Higher Order Modes on Microstrip Line," IEEE MTT–S Microwave Symposium Digest, 1986, pp. 57–60.

[5] Kasilingam, D. P. and D. B. Rutledge, "Surface–Wave Losses of Coplanar Transmission Lines," IEEE MTT–S Microwave Symposium Digest, 1983, pp. 113–116.

[6] Mosig, J. R. and F. E. Gardiol, "General Integral Equation Formulation for Microstrip Antennas and Scatterers," IEE Proceedings, Vol. 132, Pt. H, No. 7, 1985, pp. 424–432.

[7] Rautio, J. C. and R. F. Harrington, "An Electromagnetic Time–Harmonic Analysis of Shielded Microstrip Circuits," IEEE Trans., MTT–35, 1987, pp. 726–730.

[8] Jansen, R. H., "High–Order Finite Element Polynomials in the Computer Analysis of Arbitrarily Shaped Resonators," AEU, Vol. 30, 1976, pp. 71–79.

[9] Jackson, R. W. and D. M. Pozar, "Microstrip Open–End and Gap Discontinuities," IEEE Trans., MTT–33, 1985, pp. 1036–1042.

[10] Jackson, R. W. and D. W. Matolak, "Surface to Surface Transition via Electromagnetic Coupling of Coplanar Waveguides," IEEE Trans., MTT–35, 1987, pp. 1027–1032.